Green synthesis of Ag-ZnO nanocomposites using leaf extract *Ipomoea Indica* and its photocatalytic dye degradation and Antibacterial Activity

Igneshgrace A[1], E.Sindhuja[1*]

[1]*PG and Research Department of Chemistry, Sri Paramakalyani College, Alwarkurichi, Affiliated to ManonmaniamSundaranar University, Abishekapatti, Tirunelveli, Tamil Nadu, India.*

Corresponding author: sindhujaelangovan@gmail.com

ABSTRACT

In recent years, the green synthesis metal oxide nanoparticles using various plant extracts has attracted great attention. This is because; these methods are simple, inexpensive and, eco-friendly. In this research work mainly have focused on the green synthesis of silver nanoparticles (AgNPs) and zinc oxide nanoparticles (ZnONPs) and Ag coated with ZnO nanocomposite (Ag/ZnO) by using leaf extract of *Ipomoea Indica* (II) as reducing and stabilizing agent. Silver nitrate ($AgNO_3$) and Zinc acetate dihydrate ($Zn(CH_3COO)_2.2H_2O$), are the forerunners in the hydrothermal Synthesis. The prepared AgNPs, ZnONPs, and Ag/ZnO nanocomposite were characterized using various instrumental techniques such as Fourier Transform-Infrared spectroscopy (FT-IR), UV-visible spectroscopy (UV-Vis), X-ray diffraction pattern (XRD) and Scanning electron microscope (SEM), Energy dispersive X-ray analysis (EDAX), High Resolution-Transmission Electron microscope (HR-TEM). The results obtained that of Ag/ZnO nanocomposite were the average size 20-50 nm. The Tauc plot of Ag/ZnO nanocomposite shows lower band gap (1.73ev). Under visible light illumination, methylene blue (MB) was degraded photocatalytic studies using AgNPs, ZnONPs, and Ag/ZnO nanocomposite, which was then examined using UV-visible spectroscopy. In comparison to AgNPs (86%) and ZnONPs (81%), Ag/ZnO nanocomposite shown superior photocatalytic activity for the breakdown of MB with a high percentage degradation efficiency (90%). The photocatalytic degradation rate constant was evaluated by using a pseudo-first order kinetic equation. Additionally, the agar disc diffusion method was used to examine the antibacterial activity against two bacterial strains (Escherichia coli and Staphylococcus aureus), and a sizable zone of inhibition against the bacterial strains was found.

Keywords:*Ipomoea Indica*; Ag-ZnO nanocomposite; Photocatalytic degradation; Visible light irradiation; Methylene blue; Antibacterial studies

INTRODUCTION

Many industries, including the paper industry, the tanning of leather, and the textile industry, use synthetic colours. Significant volumes of these harmful synthetic dyes are leaked into the environment, resulting in water contamination[1].The photocatalytic approach, which uses a variety of nanomaterials to completely mineralize the dyes on its surface, is a dependable, highly sensitive, reasonably priced, and ecologically friendly method[2-5]Researchers and pollutant management are currently interested in improving photocatalytic performance by modifying electronic structural features such as charge transfer, band gap, shape, and particle size, or by doping metal and nonmetalnanomaterials[6-8].The majorities of dyes are difficult to remove and are resistant to biodegradation, heat, and light. As a result, they might remain there for a long period. Water-soluble methylene blue (MB) is a significant aromatic chemical cationic dye used in the

textile industry [9].Effluents containing dye, like MB, can harm ecosystems and public health.Various techniques, including filtration, adsorption, reverse osmosis, coagulation, solvent extraction, and photodegradation, have been employed to remove dyes from effluents.Adsorption of dyes is appealing because to its low cost, high efficiency, ease of operation, and small volume of sludge to be disposed[10]. Advance oxidation processes such as photocatalysis have recently very popularity for the removal of complex organic contaminants and dyes under visible light irradiation.Silver has been discovered to improve the photocatalytic activity of semiconductor NPs [11].

ZnO has been discovered to be useful in the degradation of industrial effluents due to its high photosensitivity, broad band width, and stability.ZnO exhibits low efficiency under solar irradiation because of its wide band gap and rapid electron-hole recombination [12].Recent studies suggest that the addition of noble metal nanoparticles to the ZnO surface, such as Pd [13], Pt [14], Ag [15–22] and Au [23] increases the photocatalytic reactivity in the degradation of different organic dyes.Metallic silver nanoparticles among noble metals exhibit great effectiveness in enhancing the photocatalytic activity of ZnO due to their low cost in compared to other noble metals such as Au, Pt, and Pd [24].The homogeneousdispersion of metallic silver nanoparticles on the ZnO surface requires a mildreduction process.

Green synthesis has been proposed as a valuable alternative path to chemical methods for the synthesis of nanoparticles using natural sources such as microorganisms, plants, or plant extracts[25-28].Among these, the use of plant extracts has generated a great deal of interest in the synthesis of nanoparticles.Plant biodiversity has been widely used for green synthesis due to the existence of useful phytochemicals such as ascorbic acids, phenols, carboxylic acids, terpenoids, amides, flavones, aldehydes, ketones, sugars, flavones, and so on. The natural extract is high in bioactive chemicals that are expected to bind to the surface of nanoparticles [29]. Because of their low toxicity and environmental safety, these qualities make them suitable for biomedical applications such as medication administration, anti-bacterial, biosensors, food packaging, and photochemical water splitting [30].The metal-metal oxide nanocomposites have drawn increased attention in the research community because when metal oxides and metals are coupled, a schottky barrier is created as the metal oxide electrons flow towards the metal until equilibrium is reached, causing the conduction band to bend.

The present study describes the synthesis of Ag–ZnO nanocomposite using leaf extract of neem prepared by a hydrothermal approach.The driving motive for this work is to study whether the *I. Indica* leaf plant extract can be used as the reducing and stabilizing agent in the synthesis of Ag–ZnO nanocomposite, thereby avoiding toxic chemicals.Under the influence of visible light, the produced metal and metal oxides nanocomposite were examined and used for the photocatalytic degradation of MB blue dye. Under visible light irradiation, Ag-ZnO nanocomposite demonstrated a good photocatalytic degaradation of MB. The materials were also examined for antibacterial

activity against Gram-positive and Gram-negative bacteria, including *Escherichia coli* and *Staphylococcus aureus*. The results of the experiment demonstrated that Ag-ZnO exhibited superior antibacterial activity than AgNPs and ZnONPs against the germs *S. aureus* and *E. coli*. Moreover, the effects of silver doping on the properties of zinc oxide are also studied using various characterization tools like Fourier Transform Infrared spectroscopy (FTIR), UV-visible spectroscopy,X-Ray Diffraction (XRD), Scanning Electron Microscope (SEM), Energy Dispersive X-Ray Spectroscopy (EDS) and Transmission Electron Microscope (TEM).

2.0 EXPERIMENTAL SECTION

2.1 Chemicals reagents

Ipomoea Indica(leaves) were obtainedManjolai, Tirunelveli, in Tamil Nadu, India. Analytical gradeSilver nitrate ($AgNO_3$ 99%) Zinc acetate dihydrate ($Zn(CH_3COO)_2.2H_2O$ 99%), Methylene blue ($C_{16}H_{18}ClN_3S$) and ethanol were purchased from Sigma Aldrich Bangalore in India.Throughout the experiment, deionized water (DW) was used for washing and solution preparation.

2.2 Preparation of Plant Extract

The leaves of Blue Morning Glory commonly known as*Ipomoea Indica*, were cleaned with distilled water and dried for two days to remove moisture.. Then the leaves were dried, powdered and protected with an air bag. Heat 2.0 g of *I. indica*powder in 250 mL of distilled water with constant stirring at 80°Cfor 1hr. The extract was filtered after cooling and kept at 4 °C for use in upcoming investigations.

2.3 Synthesis of AgNPs and ZnONPs

Preparation of AgNPs: 4.0 g (0.05M) of $AgNO_3$ was stirred in 80 mL distilled water for 30 minutes and then added to 10 mL of extract and the solution was stirred for another 30 min. Then mixture of the solution was transferred into 100 mL, Teflon coated autoclave and heated in muffle furnace at 180°C for 6 hrs. After cooling the solution was centrifuged at 6000 rpm for 15 min to obtain a black precipitate, and then washed several times with water and ethanol to remove impurities. The precipitate was then dried at 100 °C to obtain a black powder. ZnONPs were also synthesized under the above condition.

2.4 Synthesis of Ag-ZnO nanocomposite

0.1M (2.0 g) of $AgNO_3$, 0.1M (2.0 g) $Zn(CH_3COO)_2.2H_2O$ of were added 80 mL distilled water and addition of 20 mL of extract solution was added and the solution is stirred for another 30 minutes at room temperature to obtain a homogenous mixture solution. The mixture was then poured into 100 mL Teflon coated autoclave and heated at 180 °C for 6hrs. After cooling the solution to room temperature, solution was centrifuged at 6000 rpm to obtain Ag-ZnO nanocomposite.

2.5 Characterization

The prepared nanomaterials of AgNPs, ZnONPs and Ag-ZnO nanocomposite were characterized using different instrument methods. UV-visible spectroscopy was used to characterize metal oxides and nanocomposite formation using UV-visible spectrophotometer (Hitachi UH-5300 spectrophotometer Double beam). Fourier transform infra red spectroscopy

was performed using(Nicolet IS5R FTIR, KBR windows with AR Diamond crystal plate, Make: Thermofisher) for identify the function group in extract and metal oxides bond interaction.Crystalinity and phase purity of X-ray diffractometers (Bruker Eco D8 Advance) were investigated.The surface morphology and shape of metal oxide and metal oxides nanocomposite was studied by SEM (vega 3 Tescan). The elemental composition of metal oxides and metal oxide nanocomposite was determined by Energy-Dispersive X-ray (vega 3 Tescan).Using HR-TEM (Jeol, JEM 2100), the NPs' morphology was evaluated.

2.6 Photocatalytic degradation method

Under visible light irradiation from a source of (250 W Xenon lamp, intensity 400 mW cm-2), photocatalytic degradation of MB with AgNPs, ZnONPs, and Ag-ZnO nanocomposite was carried out. 10 ppm of MB in 100 mL water and 100 mg of AgNPs, ZnONPs, and Ag-ZnO nanocomposite were used as photocatalysts into the 1L glass tube. The center of the quartz glass tube was connected to a light lamp. The solution was kept under dark conditions for 30 min before visible light was illuminated to reach absorption-desorption equilibrium on the photocatalyst.This experiment was carried out at room temperature with visible light illumination. 10 mL of the degradation solution was collected at various time intervals with 0.45µM syringe filter to remove the photocatalysts. The concentration of the MB degradation solution was evaluated by using a UV-visible spectrophotometer. The absorption peak of MB was determined at 664 nm [31].The percentage degradation efficiency of MB was estimated using the following equation,

$$D\ (\%) = C_0\text{-}C_t/C_0 \times 100 \quad \text{..... (1)}$$

Where C_0 and $C_t$represent the MB dye solution's initial and final concentrations over time, respectively.

2.7 Anti-bacterial assessment

The tools for the experiment were placed in an autoclave for 20 minutes at 121 °C. Before usage, *Escherichia coli* (*E.coli*) and *Staphylococcus aureus* (*S.aureus*) cultures were cultured in 50 ml of nutrient broth (NB) and incubated at 37 °C overnight before being used. The disc diffusion method was used to test the antibacterial activity of synthesisedAgNPs, ZnONPs, and Ag-ZnO nanocomposite. After adding 20 ml of sterile Mueller Hinton Agar, 120 ml of bacterial culture was poured onto sterile petri plates and dispersed around with a spreader. On a 6 mm sterile disc, AgNPs, ZnONPs, andAg-ZnO nanocomposite were deposited. The loaded disc was placed on the medium's surface, and the extract was allowed to diffuse for five minutes before the plates were incubated for 24 hours at 37 °C. As a control, E.coli and Staphylococcus aureus (S.aureus) bacteria were mixed in with the solvents. [32,33]. The inhibitory zones that had formed around the disc were measured in millimeters using a transparent ruler at the end of the incubation period.

3. RESULT AND DISCUSSION

3.1. UV-Visible Characterisation.

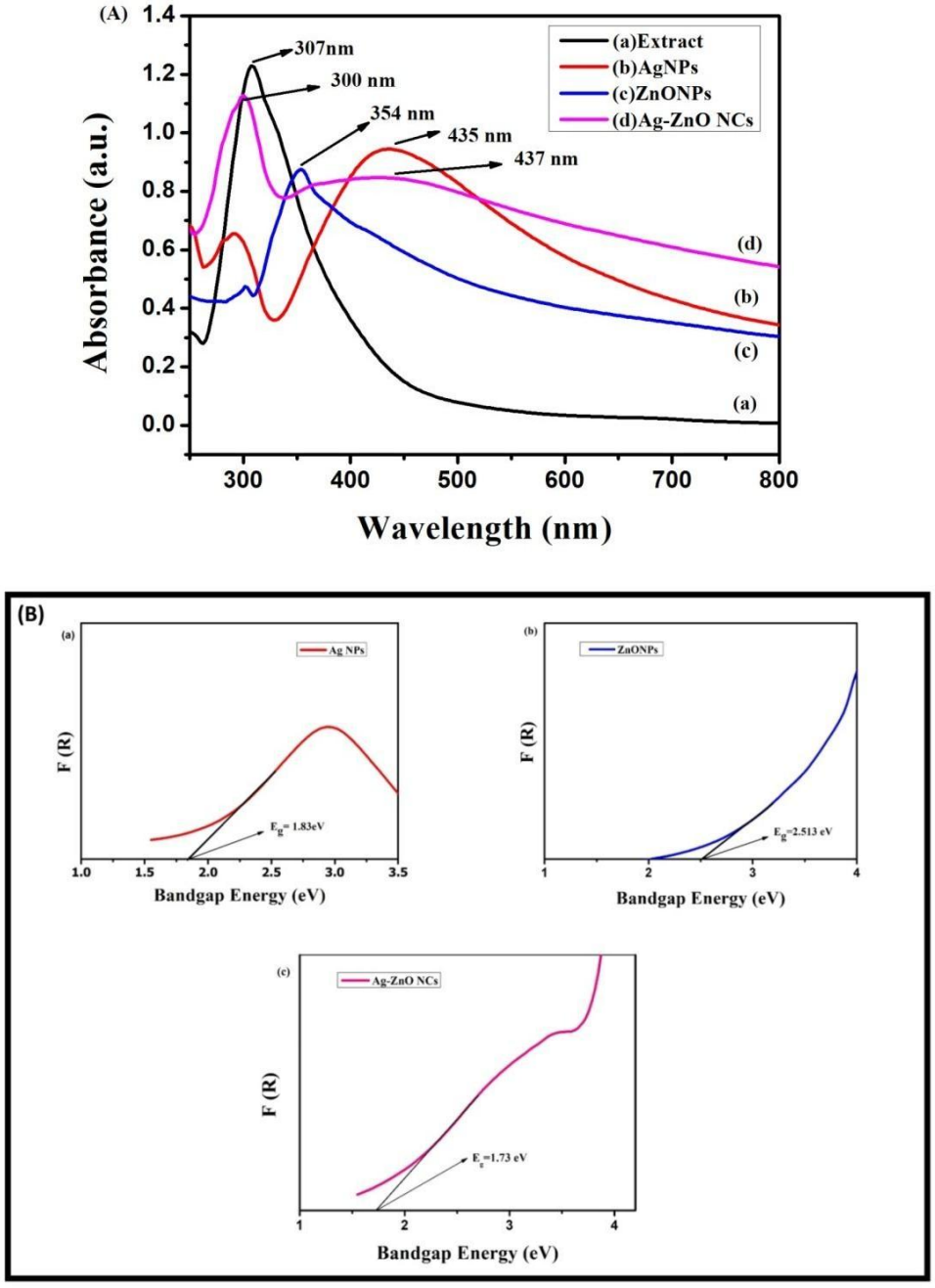

Figure1(A,B): (A) UV–Visible absorption spectra of (a) Extract, (b) AgNPs, (c) ZnONPs, (d) Ag-ZnO NCs and (B) Tauc plot of (a) AgNPs, (b) ZnONPs, (c) Ag-ZnO NCs

Figure 1A (a-d) shows the UV-visible spectra of *I. Indica*extract, AgNPs, ZnONPs and Ag/ZnO nanocomposite. Peaks at 307 nm appeared in the *I. Indica*extract due to the presence of the polyphenolic compounds as shown in Fig.1A (a) [34]. A broad band at 435nm indicated at the presence of AgNPs as shown in Fig.1A (b). The presence of a strong band at 354nm indicated the synthesis of ZnONPsas shown in Fig.1A (c) [35]. In the case of Ag-ZnO nanocomposite using Ipomoea indica leaf extract, the maximum absorption peaks were observed at 300 nm and another peak was obtained at 437 nm, confirming that the interaction between silver and Zinc Oxide [36].Figure 1B (a-c) shows the Tauc plot of AgNPs, ZnONPs and Ag-ZnOnanocomposite, where the Ag-ZnOnanocomposite (1.73 eV) has a less band gap energy than the AgNPs (1.83 eV) and ZnONPs (2.51 eV). The reduced band gap energy of the Ag-ZnO nanocomposite resulted in high photocatalytic degradation activity when exposed to visible light [37].

3.2 FT-IR Characterization

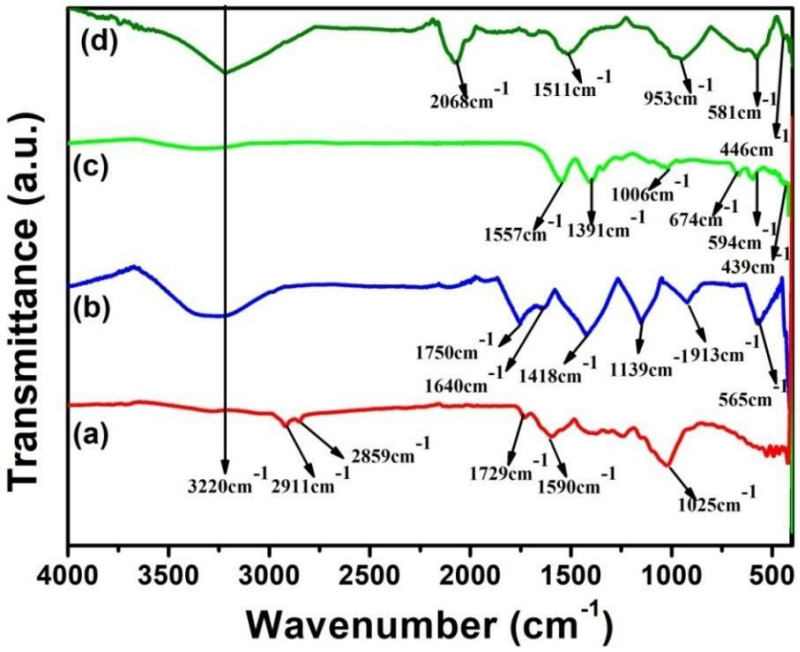

Figure2(a-d): FT-IR spectra of(a) Extract, (b) AgNPs, (c) ZnONPs, (d) Ag-ZnO NCs

The FT-IR spectra of *I. Indica*extract, AgNPs, ZnONPs and Ag/ZnOnanocomposite is shown in Fig.2 (a-d).Fig.2(a) shows the peaks at 3220 (O-H stretching vibration) 2911cm^{-1} and 2859 cm^{-1} (C-H stretching vibration), 1729cm^{-1} (C=O stretching vibration),1590cm^{-1} (C=C stretching vibration) and 1025cm^{-1} (C-O stretching vibration) show the presence of various functional groups in *I. Indica*extract [38]. Fig.2(b) showsthe peaks of 1750cm^{-1} (C=O stretching vibration),Silver has distinctive peaks at around 1136 cm-1, 1418 cm-1, and 1640 cm-1, 913cm^{-1}and 565cm^{-1}[39,40]. Fig.2(c) shows the peak at 1557cm^{-1} is attributed to C=C stretch of benzene and amide linkage, the peaks at 1391cm^{-1}indicates the presence of C-N stretching, The peak at 1006 cm-1 is attributed to the stretching vibration of the C-O bond. The adsorption peaks appearing at 594cm^{-1}439cm^{-1}is due to the stretching mode of the metal and oxygen bond (ZnO stretching vibrations) [41-43].The figures clearly show that the intensity of the peaks increases in the case of the Ag-ZnO nanocomposite.

3.3 XRD Characterization

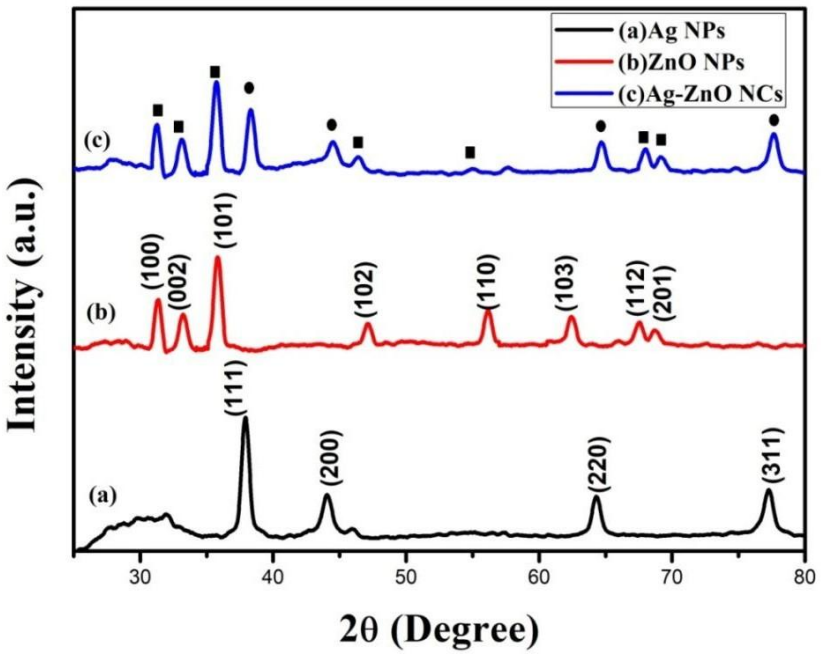

Figure3(a-c) X-ray spectra of (a) AgNPs, (b) ZnONPs, (c) Ag-ZnO NCs

X-ray diffraction (XRD) method is used to identify the crystalinity of nanomaterials. X-ray diffraction pattern of *I. Indica* Extract, AgNPs, ZnONPs and Ag-ZnOnanocomposite areshown in Fig.3 (a-c).The XRD pattern (Fig.3(a)) revealed a number of Bragg reflections that may be indexed using the face-centered cubic structure of silver. It proved that the silver particles generated in our studies were nanocrystals, as demonstrated by the peaks at 2θ values of 37.8 °(111), 44.03 ° (200), 64.25°(220), and 77.24 °(311). The results show that the nanoparticles were face-centered cubic in structure (JCPDS file nos. 84-0713 and 04-0783)[44].Fig.3(b) shows the diffraction peak of ZnO NPs at(100), (002), (101) (102) (110), (103) ,(112) and (201) crystals with scattering angles of 31.4°, 33.14°, 35.86°, 47.07°, 56.29°, 62.47°, 67.60° and 68.76 with corresponded to a hexagonal ZnO phase (wurtzite structure) (JCPDS 36-1451) [45].Fig. 3(c) show the ZnO phase is represented by the six main peaks displayed at 2 θ values: 31.3, 33.4, 35.6, 46.4, 55.0, 67.7, and 69.1 (marked as ■). Meanwhile, the four significant peaks at 2θ values of 38.28, 44.56, 64.78, and 77.76 (marked as ●) can be attributed to the Ag phase. According to the XRD data, the product generated through green synthesis using*I. Indica*extract is a complex composed of Ag and ZnO nanoparticles. As a consequence of the XRD data, Ag-ZnO nanocompositesuccesfully formed by the hydrothermal synthesis process [46]. Using Scherrer's equation, the average particle sizes of the samples are calculated from the full-width half maximum (FWHM) of the most intense diffraction peaks.

$$D = K\lambda/\beta \cos \theta \text{.....(2)}$$

Where k is Scherrer's constant (0.9), λ is X-ray wavelength (1.54×10^{-10} m), β is Full Width at Half Maximum, and h is Bragg's angle. The average particle diameters for Ag, ZnO, and Ag-ZnO nanoparticles are 15 nm, 23 nm, and 25 nm, respectively.

3.4 Scanning Electron Microscope (SEM) characterization

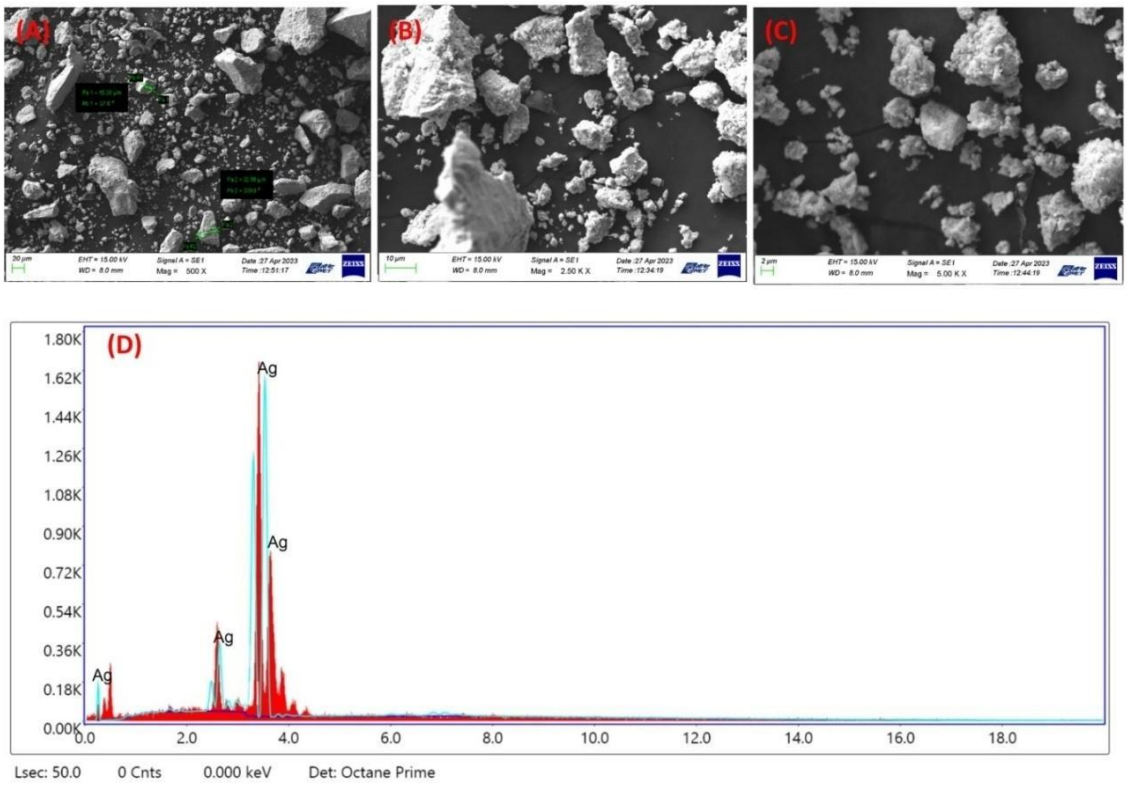

Figure4 (A-D):SEM images ofAgNPs(A) 20 µM, (B) 10 µM, (C) 2 µM and (D) Energy dispersive spectra (EDX).

SEM analysis is used to investigate the morphological structures of the synthesized nanoparticles.The surface morphology of the AgNPs study was examined by SEM at different magnifications of 20µM, 10 µM and 2 µM in Fig.4 (A–C). Low magnification white agglomerate particles were obtained at 20 µM, as illustrated in Fig.4 (A).As indicated in Fig. 4 (B&C), very compact spherical particles were seen at higher magnification at 10 and 2 µM.Fig.4 (D) displays the elemental composition of the nanoparticles examined using an EDX spectrum.The EDX spectrum of AgNPs sample confirms the presence only silver which is evidenced for the preparation of impurity free nanoparticles of Ag.

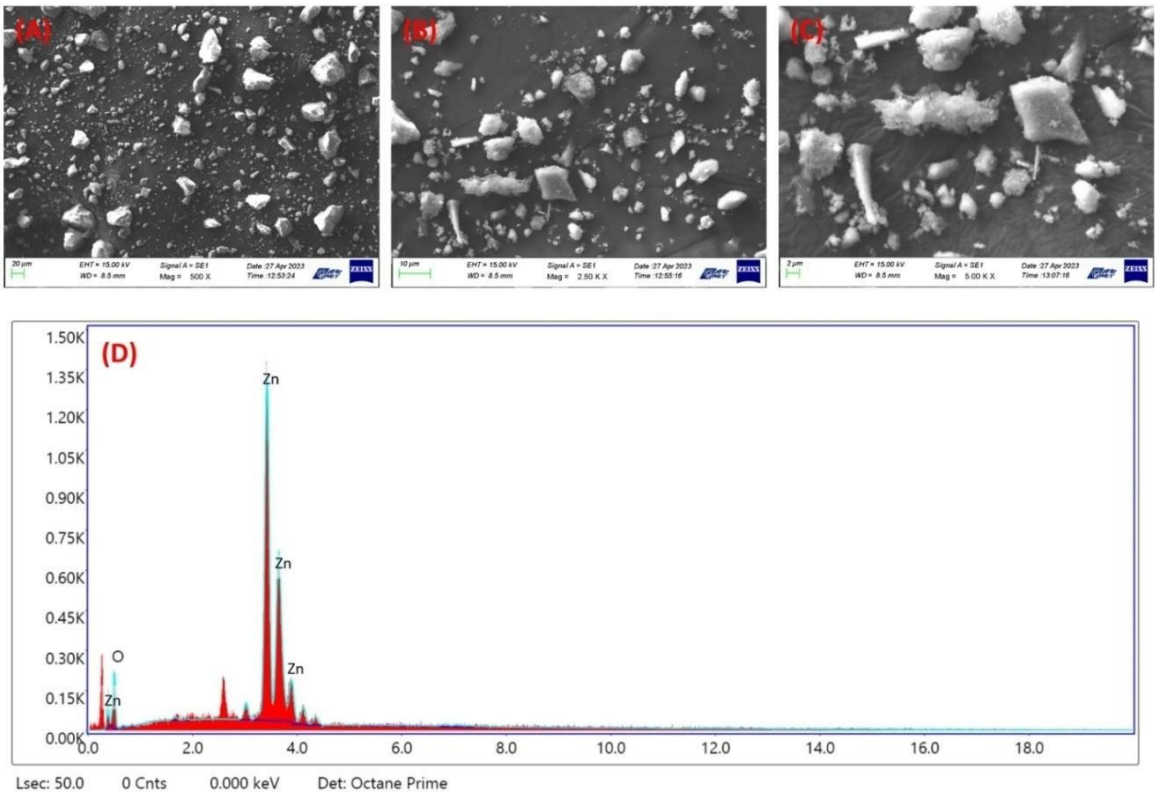

Figure5 (A-D):SEM images ofZnONPs(A) 20 µM, (B) 10 µM, (C) 2 µM and (D) Energy dispersive spectra (EDX).

Figure5 (A-C) shows SEM images of ZnONPs characterized at 20 µM, 10 µM and 2 µM with different magnifications.The results showed fig.5 (A) that the particles in the sample were compactly packed and showed a spherical shape [47].Higher magnification Fig.5 (B) reveals that the particles are bound together by weak physical forces.Sphere like structures was clearly captured at the highest magnification 2 µM as shown in Fig.5 (C).As shown in Fig.5 (D), energy dispersive x-ray analysis (EDAX) revealed the presence of Zn, and O in ZnONPs

.

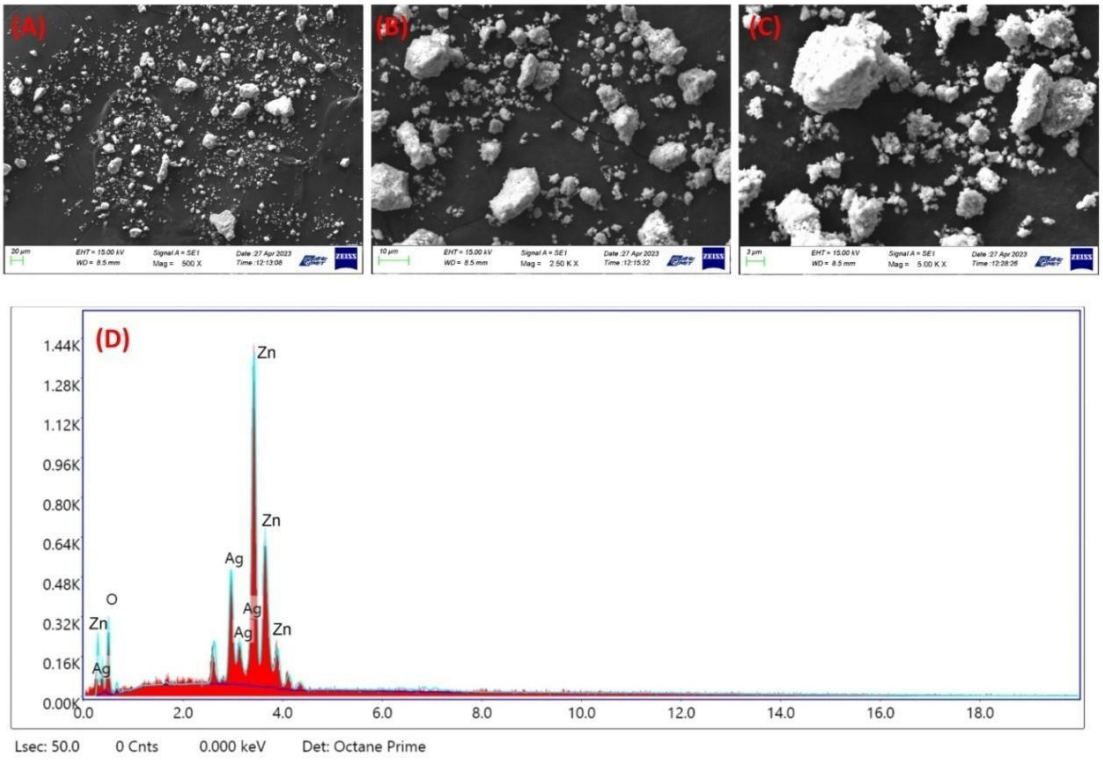

Figure6 (A-D):SEM images of Ag-ZnO NCs (A) 20 µM, (B) 10 µM, (C) 2 µM and (D) Energy dispersive spectra (EDX).

The surface morphology of the AgNPs study was examined by SEM at different magnifications of 20µM, 10 µM and 2 µM in Figure 4 (A–C).Fig.6 (A and B) arelow magnification SEM images of the Ag-ZnO nanoparticles. It Indicates the particles are agglomerated Ag/ZnO NPs.Higher magnification SEM pictures Fig. 6(C) demonstrate that the morphological structure of Ag-ZnO nanoparticles is almost spherical in shape.Larger nanoparticles form as a result of van der Waals clusters of smaller entities and magnetic interactions between the particles[48].The presence of silver, zinc, and oxygen in the EDX spectrum Fig. 6(D) from the Ag-ZnO sample verifies the synthesis of impurity-free Ag-ZnO nanoparticles.

3.5 Transmission Electron Microscope

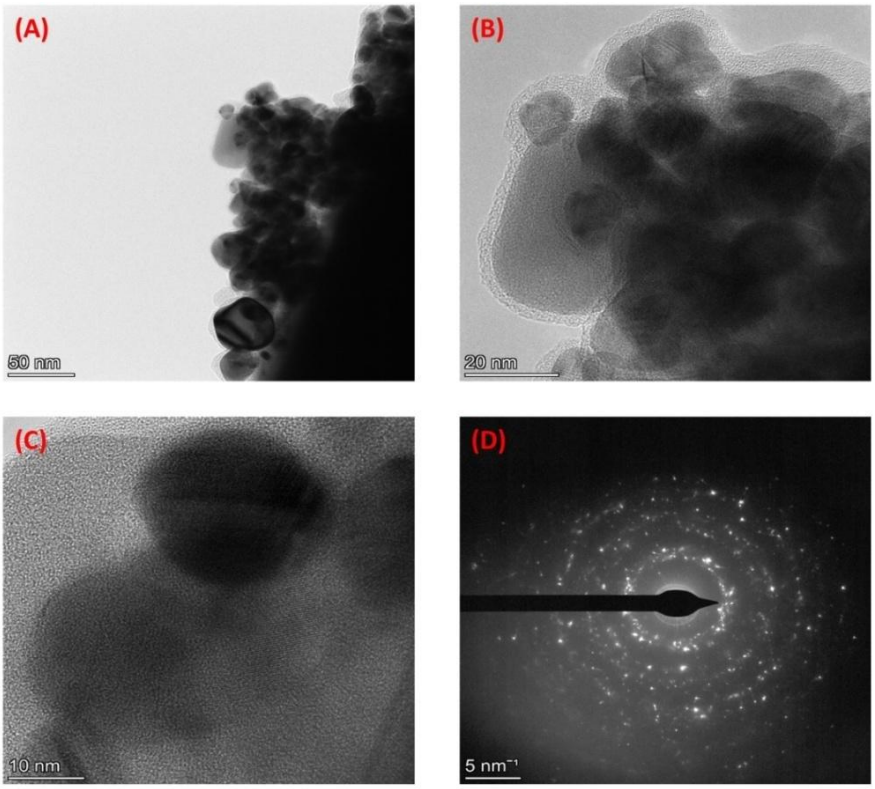

Figure7 (A-D): TEM images of the Ag-ZnO nanocomposite (A) 50 nm, (B) 20 nm, (C) 10 and (D) SAED pattern of CuO/ZnOnancomposite.

TEM images (Fig.7 (A-C)) show the shape and particle size of Ag-ZnO nanoparticles prepared by hydrothermal method,As shown in Fig.7 (A&B). The TEM images of Ag-ZnO nanocomposite have a round, spherical shape with an average particle size observed at 50 and 20nm. At higher magnification, Fig.7(C) clearly shows a large number of tiny and spherical Ag NPs 10nm deposited on the ZnO surface. It can be seen that Ag nanoparticles are anchored on the surface of ZnO, and well distributed over the surface[49].As demonstrated in Fig.7 (D), the SAED pattern confirmed the crystallinity of the Ag-ZnO nanocomposite.

3.6 Photocatalytic dye degradation

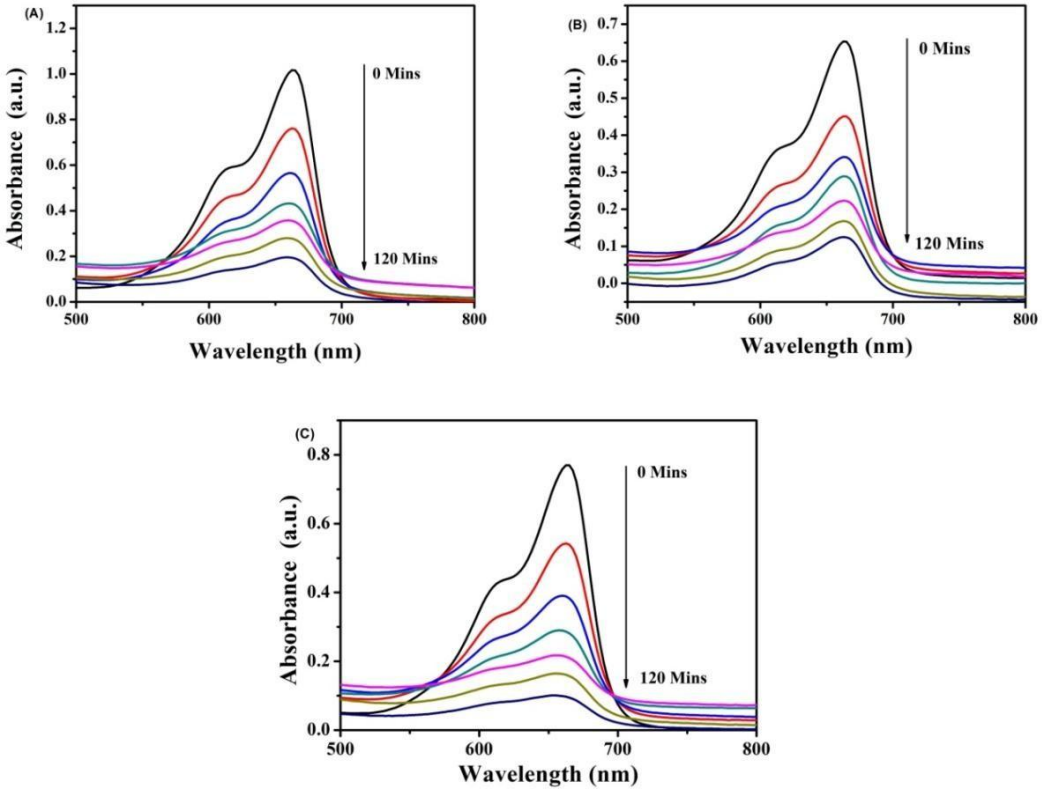

Figure8. UV-vis spectra of (A) AgNPs, (B)ZnONPs and (C) Ag-ZnO nanocomposite the photocatalytic degradation of MB under visible light irradiation at various time intervals 0 to 120 min.

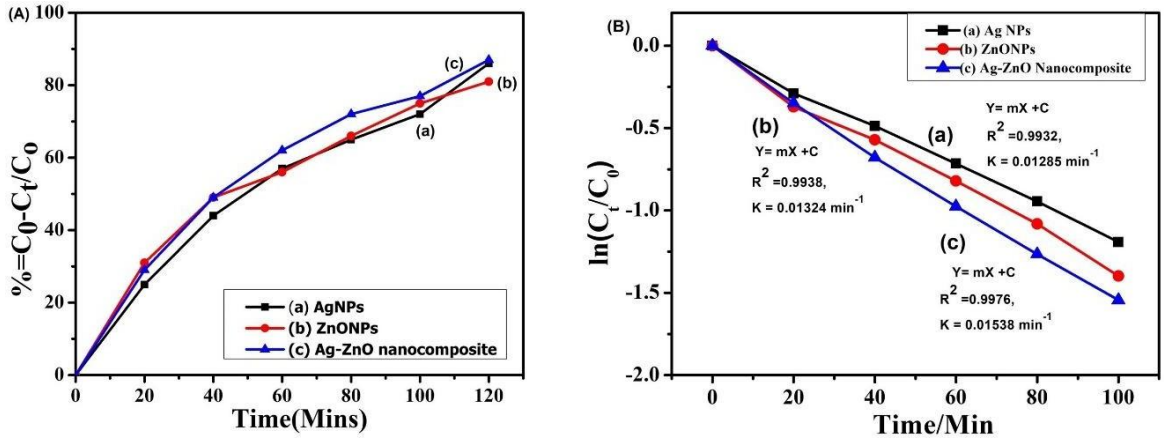

Figure9. (A) Calibration plot of the degradation efficiency vs time and (B) plot of $\ln(C_t/C_0)$ vs time.

As shown in Fig.8 (A-C), the photocatalytic degradation of MB was measured using various photocatalysts such as AgNPs, ZnONPs, and Ag-ZnO nanocomposite with visible light irradiation at different time intervals.UV absorbance was measured at 664 for the catalytic activity of Ag, ZnO, and Ag-ZnO on the photodegradation of MB.Under dark conditions, the photocatalyst of AgNPs, ZnONPs, and Ag-ZnO nanocomposite absorbed the MB dye solution first.ZnONPs were shown in Fig. 8(A) to be a photocatalyst for the degradation of MB under visible light irradiation from 0 to 60 minutes, and its peak intensity was not entirely degraded.As shown in Fig. 8(B), AgNPs practically completely degrade MB dye under visible light across time intervals ranging from 0 to 120 minutes.As demonstrated in Fig.8(C), Ag-ZnO nanocomposite conducted superior photocatalytic degradation of MB under visible light irradiation from 0 to 120 minutes [50,51]. The efficiency of photocatalytic degradation was calculated by using above equation (1).The efficiency of Ag, ZnO, and Ag-ZnO degradation for MB is displayed versus time in Fig. 9(A-C). The degradation percentage increases with exposure duration, silver doped ZnO has a better photodegradation efficiency than AgNPs and ZnONPs[49,52].The first-order rate equation was used to calculate the decomposition kinetics rate constant of MB dye with various photocatalysts of AgNPs, ZnONPs, and Ag-ZnO nanocomposite [53,54].

$$(C_t/C_0) = -kt \quad \text{.....(3)}$$

Where C_0 and C_t are the initial and final concentrations at 0 min and time t respectively, Kinetic rate constant (K, min^{-1}). K was calculated from the slope of the plot $ln(C_t/C_0)$ vs time t as shown in Fig.9B(a-c).Fig.9B (a-c) shows that Ag-ZnO NCs have a higher rate constant (K= 0.01538 min-1) than AgNPs (K= 0.01285 min-1) and ZnONPs (0.01324 min-1).

3.7 Photocatalytic dye degradation Mechanism of Ag-ZnO

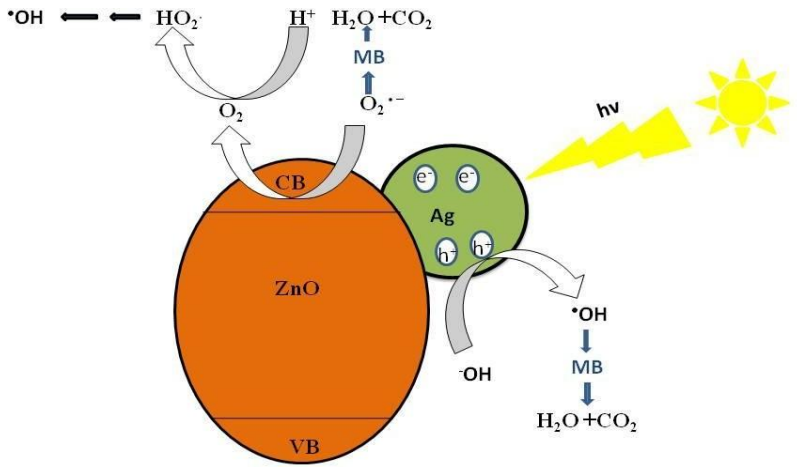

Figure 10. Photocatalytic Degradation Mechanism of MB by Ag-ZnO Nanocomposite under Visible Light Irradiation.

The photocatalytic process for Ag/ZnO under sun irradiation can be explained by the following proposed mechanism (shown in Fig. 10). When silver nanoparticles are exposed to sunlight, electron-hole pairs are formed as a result of visible light absorption via surface plasmon resonance (Eq. 4). The silver nanoparticlesplasmon-induced electrons are then rapidly pumped into the ZnO CB (Eq. 5). The trapped ZnO electrons and Ag trapped holes then react with the preadsorbed oxygen (Eq. 6) and surface-bound hydroxyl groups (-OH) (Eq. 7) to produce hydroxyl radicals. Finally, MB is degraded by hydroxyl radicals by hydrogen abstraction and subsequent oxidation processes (Eq. 8) [55-57].

$$Ag + h\nu(\text{visible light}) \rightarrow h^+ + e^- \quad (4)$$

$$Ag\ (e^-) + ZnO \rightarrow ZnO\ (e_{CB}^-) + Ag\ (h^+) \quad (5)$$

$$ZnO\ (e_{CB}^-) + O_2 \rightarrow ZnO + {}^{\bullet}O_2^- \quad (6)$$

$$Ag\ (h^+) + OH^- \rightarrow Ag + \bullet OH$$

$$\bullet O_2^- + MB \rightarrow \text{degraded products} + H_2O + CO_2 \quad (7)$$

$$\bullet OH + MB \rightarrow \text{degraded products} + H_2O + CO_2 \quad (8)$$

3.8 Anti-bacterial activity of the samples

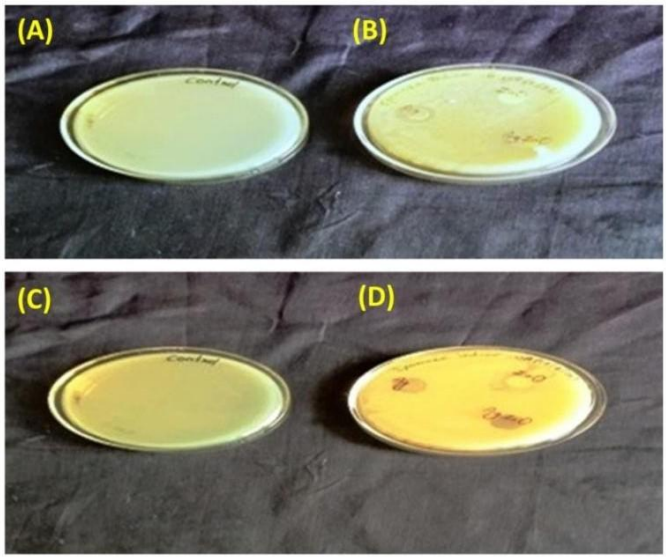

(E)

Pathogenic bacteria	Control	AgNPs	ZnONPs	Ag-ZnO NCs
E.coli	-	15mm	19mm	21mm
S.aureus	-	14mm	15mm	18mm

Figure 11. (A-E). Anti-bacterial activities of theAgNPs, CuONPs, Ag-ZnO nanocomposite samples against *E. coli (A&B)* and *S. aureus* (C&D) and (E) Comparison Result.

Disc diffusion was used to investigate the anti-bacterial activity of AgNPs, ZnONPs, and Ag-ZnO nanocomposite samples against Escherichia coli (E.coli) and Staphylococcus aureus (S.aureus) bacteria. The bactericidal activity of the samples in the presence of 120 g/mL are shown in Fig.11 (A-D). As previously stated, the AgNPs and ZnONPs samples had decreased anti-bacterial effectiveness against both Escherichia coli (E.coli) and Staphylococcus aureus (S.aureus) bacteria with Zone of (14 mm AgNPs and 15 mm ZnONPs for S.aureus and 15 mm AgNPs and 19 mm ZnONPs for E. coli). To diminish antibacterial activity, AgNPs and ZnONPs were produced using *I.Indica* extract. Surprisingly, Ag-ZnO nanocomposite demonstrated superior anti-

bacterial activity against both Zone of (E.coli for 21 mm) and (S.aureus for 18 mm).

4.0 Conclusion

Green synthesis of Ag-ZnOnanocomposite was effectively prepared by using *I. indica*(II) with the hydrothermal method. It was applied for the photocatalytic decompose of MB under visible light illuminate. FT-IR spectra confirmed the formation of Ag and Zn-O bonds in the Ag-ZnOnanocomposite. Tau's plot displayed that Ag-ZnOnanocomposite has lower band gap energy (E_g = 1.46 eV). SEM image clearly indicated that theAgO particles coated on ZnO. TEM result showed Ag-ZnO nanocomposite was slightly agglomerated in spherical shape with size around 20–50 nm. The effective degradation of MB with Ag-ZnOnanocomposite was better responded to under visible light irradiation at 90% in 120 min. Furthermore, the Ag-ZnO nanocomposite exhibited successful antibacterial action adjacent to both gram-positive and gram-negative bacteria. Consequently, it is projected that the *I. Indica* extract Ag-ZnO nanocomposite can perform as competent nanomaterials for sustainable biological and photocatalytic applications.

Acknowledgement

We thank DST-FIST, India for the IR and UV instrumental facilities at the PG and Research centre, Department of Chemistry, Sri Paramakalyani College, Alwarkurichi. We thank Dr. G. Ramanathan,Deparment of Microbiology, SriParamakalyani College for antibacterial studies.

Conflicts of interest

The authors declare no conflict interest.

REFERENCE

1. Forgacs E, CserhatiT,OrosG,Removal of synthetic dyes from wastewaters: a review. Environ. Int. **2004**, 30(7), 953.
2. Zangeneh H, Zinatizadeh A. A. L, Habibi M, Akia M. & Isa, M. H. Photocatalytic oxidation of organic dyes and pollutants in wastewater using different modified titanium dioxides: a comparative review. J. Ind. Eng. Chem.**2015**,26, 1–36.
3. Mingxin L, Photocatalytic performance and mechanism research of Ag/HSTiO2 on degradation of methyl orange. ACS Omega**2020**, 5, 21451–21457.
4. Guan R, Zhai H, & Sun D. Effects of Ag doping content and dispersion on the photocatalytic and antibacterial properties inZnO nanoparticles. Chem. Res. Chin. Univ. **2019**, 35, 271–276.
5. Jiaxin L.Preparation and photocatalytic performance of dumbbell Ag2CO3–ZnO heterojunctions. ACS Omega,**2020,** 5, 570–577.
6. Liu G.Unique electronic structure induced high photoreactivity of sulfur-doped graphiticC3N4. J. Am. Chem. Soc.**2010**, 132, 11642–11648.
7. Haibin L, Xuechen D, Guocong L. &Xiaoqi L. Photochemical synthesis and characterization of Ag/TiO2 nanotube composites.J. Mater. Sci.**2008**, 43, 1669–1676.
8. Jin, Q., Fujishima, M. & Tada, H. Visible-light-active ironoxide-modified AnataseTitanium(IV) Dioxide. J. Phys. Chem. C,**2011**,115, 6478–6483.
9. Balamurugan S, Balu AR, Narasimman V, Selvan G, Usharani K, Srivind J, Suganya M, Manjula N, Rajashree C, NagarethinamVS , Multi metal oxide CdO-Al2O3-NiO nanocompositesynthesis, photocatalytic and magnetic properties. Mater Res Express. **2019**, 6, 015022.
10. Chen H, Zhao Y. & Wang A. Removal of Cu (II) from aqueous solution by adsorption onto acid-activated palygorskite.**2007**,149**,** 346–354.
11. Wu H, Jian W, Dang H. & Zhao X. Hierarchical Ag-ZnO Microspheres with Enhanced Photocatalytic Degradation Activities.Pol. J. Environ. Stud, **2017**, 26(2), 871–880
12. PantB, Park M.Kim H.Y, ParkS.J,Ag-ZnOphotocatalyst anchored on carbon nanofibers: synthesis, characterization, and photocatalytic activities, Synth. Met. **2016**, 220, 533
13. Zhang Y,Wang Q,Xu J,Ma S,Synthesis of Pd/ZnO nanocomposites with high photocatalytic performance by a solvothermal method. Appl. Surf. Sci. **2012,** 258(24), 10104.
14. Yuan J, Choo E.S.G,Tang X,Sheng Y,Ding J,Xue J,Synthesis of ZnO–Pt nanoflowers and their photocatalytic applications,Nanotechnology **2010**, 21(18),185606.
15. Han Z,Ren L,Cui Z, Chen C, Pan H, J. Chen. Ag/ZnO flower heterostructures

as a visible-light driven photocatalyst via surface Plasmon resonance, Appl.Catal. B **2012**,126, 298.

16. Cai T, Wang L, Liu Y, Zhang S, Dong W, Chen H, Yi X, Yuan J, Xia X, Liu C, Luo S, Ag_3PO_4/Ti_3C_2 MXene interface materials as a Schottky catalyst with enhanced photocatalytic activities and anti-photocorrosion performance,Appl. Catal. B **2018,**239, 545–554
17. Cai T, Liu Y, Wang L, Zhang S, Dong W, Chen H, Ma J, Liu C, Luo V, Ultrafine Ag@AgI nanoparticles on cube singlecrystal Ag_3PO_4 (100): an all-day-active Z-Scheme photocatalyst for environmental purification,J. Colloid Interface Sci. **2019**, 533, 95–105.
18. Cai T, Liu Y, Wang L, Zhang S, Zeng Y, Yuan J, Ma J, Dong W, Liu C,LuoS, Silver phosphate-based Z-Scheme photocatalytic system with superior sunlight photocatalytic activities and anti-photocorrosion performance, Appl. Catal. B **2017,** 208, 1–13.
19. Jaramillo-PáezC, NavíoJ. A, HidalgoM. C, Silver-modified ZnO highly UVphotoactive,J. Photochem. Photobiol. A **2018**, 356, 112–122.
20. LamaS.M, QuekaJ.A, Sin J.C, Mechanistic investigation of visible light responsive Ag/ZnO micro/ nanoflowers for enhanced photocatalytic performance and antibacterial activity,J. Photochem. Photobiol. A **2018**, 353 171–184.
21. AnsariS.A, KhanM.M, LeeJ, ChoM.H,Highly visible light active Ag@ ZnO nanocomposites synthesized by gel-combustion route.Ind. Eng. Chem. Res. **2014**, 20(4), 1602.
22. RajbongshiB.M, RamchiaryA, JhaB.M, SamdarshiS.K, Synthesis and characterization of plasmonic visible active Ag/ZnOphotocatalyst.J. Mater. Sci. Mater. Electron. **2014,** 25(7), 2969.
23. TahirM.N, Natalio F, CambazM.A, Panthöfer M, Branscheid R, Kolb U, Tremel W, Controlled synthesis of linear and branched Au@ZnO hybrid nanocrystals and their photocatalytic properties**,** Nanoscale **2013,**5(20) 9944.
24. Wei D, QianW,Facile synthesis of Ag and Au nanoparticles utilizing chitosan as a mediator agent**.** Colloids Surf. B**2008,**62(1), 136.
25. Vigneshwaran N, Nachane R, Balasubramanya R, &Varadarajan P, A novel one-pot 'green'synthesis of stable silver nanoparticlesusing soluble starch. *Carbohydr. Res.* **2006,**341, 2012–2018.
26. Azizi S, Ahmad M. B, Namvar F, & Mohamad R, Green biosynthesis and characterization of zinc oxide nanoparticles usingbrown marine macroalgaSargassummuticum aqueous extract. Mater. Lett. **2014**, 116, 275–277.
27. Fahad A,Synthesis of nanocauliflowerZnOphotocatalyst by potato waste and its photocatalytic efficiency against dye. J.Mater. Sci. Mater. Electron. **2020,**31, 11538–11547.
28. Singh G,Synthesis of ZnO nanoparticles using the cell extract of the cyanobacterium, Anabaena strain L31 and its conjugation with UV-B absorbing compound shinorine. J.

Photochem. Photobiol. B Biol. **2014**,138, 55–62 .

29. PerveenR, ShujaatS, QureshiZ, NawazS, KhanM.I, IqbalM,Green versus sol-gel synthesis of ZnO nanoparticles and antimicrobial activity evaluation against panel of pathogens J. Mater. Res. Technol**2020,** 9(4) 7817–7827.
30. I. Hussain, N.B. Singh, A. Singh, H. Singh, S.C. Singh, Green synthesis of nanoparticles and its potential application, Biotechnol. Lett. **2016**,38(4), 545–560,
31. Dina F. Katowah Sayed M. Saleh Sara A. Alqarni, Reham Ali, Gharam I. Mohammed1 & Mahmoud A. Hussein, Network structure-based decorated CPA@CuO hybrid nanocomposite for methyl orange environmental remediation, Scientific Reports **2021**, 11, 5056
32. Bhuvaneswari P, Shanmugavadivu T, Sabeena G, Annadurai G, Sindhuja E. Synthesis and characterization of chitoson with silica (CS) nanocomposite with enhanced antibacterial activity, Int. J. Res. Pharm. Sci.,**2022**, 13(1), 1-8.
33. Shanmugavadiv T, Bhuvaneswari P, Sabeena G, Annadurai G, Sindhuja E. Synthesis and characterization of chitoson with monomorllonite nanocomposite (CNC) with enhanced antibacterial activity. J. Bio. &Env. Sci.**2022**, 21, 148-156
34. Yuvarani S, Selvam, Phytochemical Analysis And Antibacterial Activity Of Ipomoea IndicaPlant Leaf Extracts International Journal of Current Pharmaceutical Research **2018**, 10(2).
35. KarunakaranC, RajeswariV, GomathisankarP, Optical, electrical, photocatalytic, and bactericidal properties of microwave synthesized nanocrystalline Ag-ZnO and ZnO, Solid State Sci., **2011**, 13, 923-928.
36. Patil S.S, Patil R.H, Kale S.B, Tamboli M.S, Ambekar J.D, Gade W.N, Kolekar S. S, Kale B.B,Nanostructured microspheres of silver @ zinc oxide: an excellent impeder of bacterial growth and biofilmJ. Nano Res. **2014**, 16,2717
37. Sun T, Qiu J. & Liang C, Controllable Fabrication and Photocatalytic Activity of ZnONanobeltArrays, **2008**, 112(3), 715–721.
38. Bashir M, Waheed A, Hamid F. S, Ali S,Functional Group Analysis of Extracts of Leaf and Stem of *Ipomoea Indica*by using FTIR SpectrumJ. Adv. Res. Biochem. Pharma. **2019**, 2(2), 20-25
39. Jyoti K, Baunthiyal M. & Singh A. ScienceDirect Characterization of silver nanoparticles synthesized using Urticadioica Linn . leaves and their synergistic effects with antibiotics. J. Radiat. Res. Appl. Sci.**2016,**9, 217-227.
40. Babu A T, Antony R, Green synthesis of silver doped nano metal oxides of zinc & copper for antibacterial properties, adsorption, catalytic hydrogenation &photodegradation of aromatics, **2016**, 3437(18), 30763-2.
41. Jayarambabu N, Siva Kumari B, Venkateswara RaoK. and PrabhuY.T,Germination and Growth Characteristics of Mungbean Seeds (Vignaradiata L.) affected by

Synthesized Zinc Oxide Nanoparticles, International Journal of Current Engineering and Technology **2014**, 4(5).

42. KwonY.J, KimK.H, LimC.S, ShimK.B, Characterization of ZnOnanopowders synthesized by the polymerized complex method via an organochemical route, J. Ceram. Process. Res. **2002**, 3, 146–149
43. Aiswarya DeviS, HarshinyM, UdaykumarS,GopinathP, and MatheswaranM, Strategy of metal iron doping and greenmediatedZnO nanoparticles: dissolubility, antibacterial and cytotoxic traits, Toxicol. Res.(Camb). **2017,**6 (6), 854–865.
44. Chekuri M, Gangarudraiah S,Roopavatharam L B, Kaphle A and Chalimeswamy A,Green synthesis of Ag nanoparticles using extract of Rosa Damascena, Eur. Chem. Bull.,**2015**, 4(10),454-459.
45. Yedurkar S, Maurya C, Mahanwar P, Biosynthesis of Zinc Oxide Nanoparticles Using IxoraCoccineaLeaf Extract—A Green Approach, Open Journal of Synthesis Theory and Applications, **2016**, 5, 1-14.
46. Zare M, Namratha K, Byrappa K,Green Synthesis and Characterization of ZnO-Ag Nanocomposite by Thymus vulgarisIJSRST, **2018**, (4) 5, 1636-1640.
47. Meruvu H, Vangalapati M, Chippada S C, Bammidi S R. Synthesis and characterization of zinc oxide nanoparticles and its antimicrobial activity against bacillus subtilis and escherichia coli. Rasayan J Chem **2011**, 1, 217-22.
48. Manyasree D, Kiranmayi P, Venkata R KolliCharacterization And Antibacterialactivity Of ZnoNanoparticlessynthesized By Co Precipitation Method Int J App Pharm,**2018**,6, 224-228
49. Noohpisheh Z, Amiri H, Farhadi S,Mohammadi–gholami A,Green synthesis of Ag-ZnO nanocomposites using *Trigonellafoenum-graecum*leaf extract and their antibacterial, antifungal, antioxidant and photocatalytic propertiesSpectrochimicaActa Part A: Molecular and Biomolecular Spectroscopy**2020**, 118595.
50. Alharthi F. A, Alghamdi A A, Al- Zaqri N, Alanazi H. S,Alsyahi A A, Marghany A E, & Ahmad N, Facile one- pot green synthesis of Ag–ZnO Nanocomposites using potato peeland their Ag concentration dependent photocatalytic properties, Scientific Reports,**2020**, 10, 20229
51. Rabanal M. E,Solvothermal synthesis of Ag / ZnO and Pt / ZnO nanocomposites and comparisonof their photocatalytic behaviors on dyes degradation. Advanced power technology,**2016**, 27, 983-993.
52. Zhang P, Chen Y, Yang X, Gui J, Li Y, Peng P, Liu D, and Qiu J, Pt / ZnO @ C Nanocable with Dual-Enhanced Photocatalytic Performance and SuperiorPhotostability, Langmuir, **2017,**7b00995
53. Sabouri Z,Sabouri S,Moghaddas S S T H,Mostafapour A, Amiri M S.Darroudi

M,Facile green synthesis of Ag- doped ZnO/CaO nanocomposites with Cacciniamacrantheraseed extract and assessment of their cytotoxicity, antibacterial, and photocatalytic activity, Bioprocess and Biosystems Engineering, **2022**, 45, 1799-1809.

54. Igneshgrace A, Sindhuja E, Synthesis of NiO/CuO nanocomposites using leaf extract from Sapthodeacampanulataand its photocatalytic degradation of Methylene Blue under visible light Irradiation**,** Eur. Chem. Bull. **2023**,12(10), 7863-7886
55. Sohrabnezhad S, Seifi A, The green synthesis of Ag/ZnO in montmorillonite with enhanced photocatalytic activity**,** Appl. Surf. Sci, **2016**, 33, 386.
56. Han Z, Ren L, Cui Z, Chen C, Pan H, Chen J,Ag/ZnO flower heterostructures as a visible-light driven photocatalyst via surface plasmon resonance,Appl. Catal. B **2012**, 126, 298.
57. Bian J.C, Yang F, Li Z, Zeng J.L, Zhang X.W, Chen Z.D, Wang J,Mechanisms in photoluminescence enhancement of ZnOnanorod arrays by the localized surface plasmons of Ag nanoparticles. Appl. Surf. Sci. **2012**, 258(22), 8548.